Chaos from Inspiral Compact Binary:

Resonant Islands of Effective-One-Body Dynamics

Feng-Li Lin (NTNU)
@2022_NCTS_ATM
Based on 2206.10966 with **Che-Yu Chen** (ASIOP) & **Avani Patel** (NTNU)

Special thanks for **Hsu-Wen Chiang** for helpful discussions!

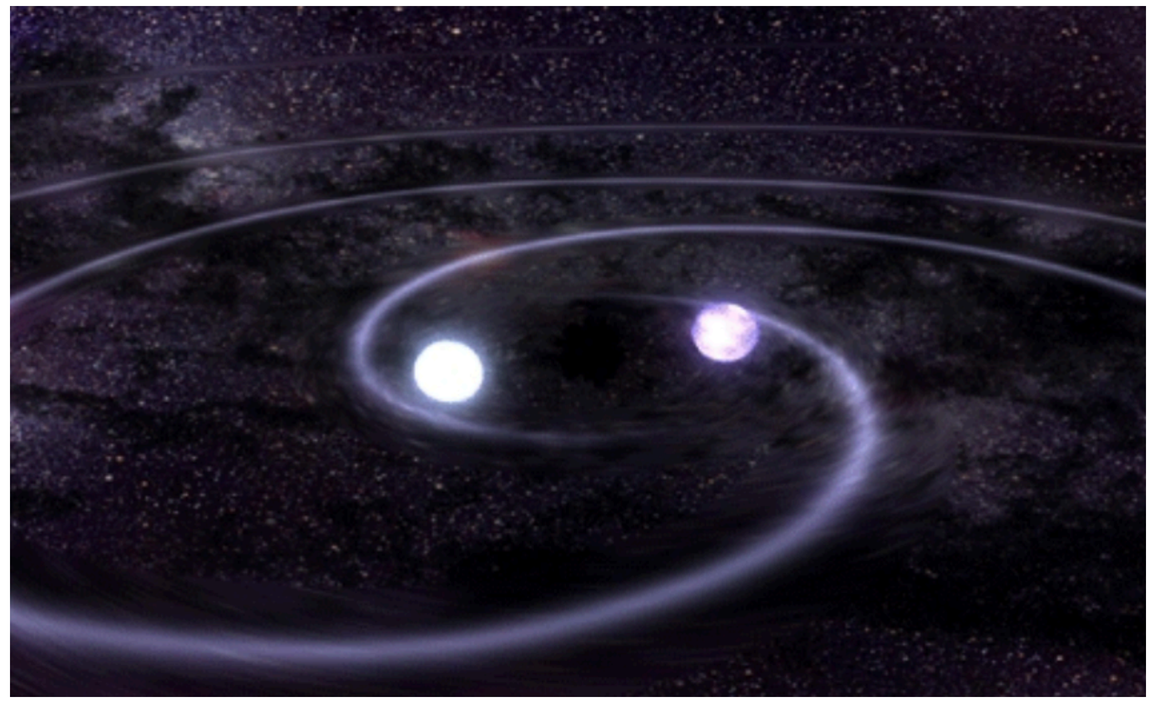

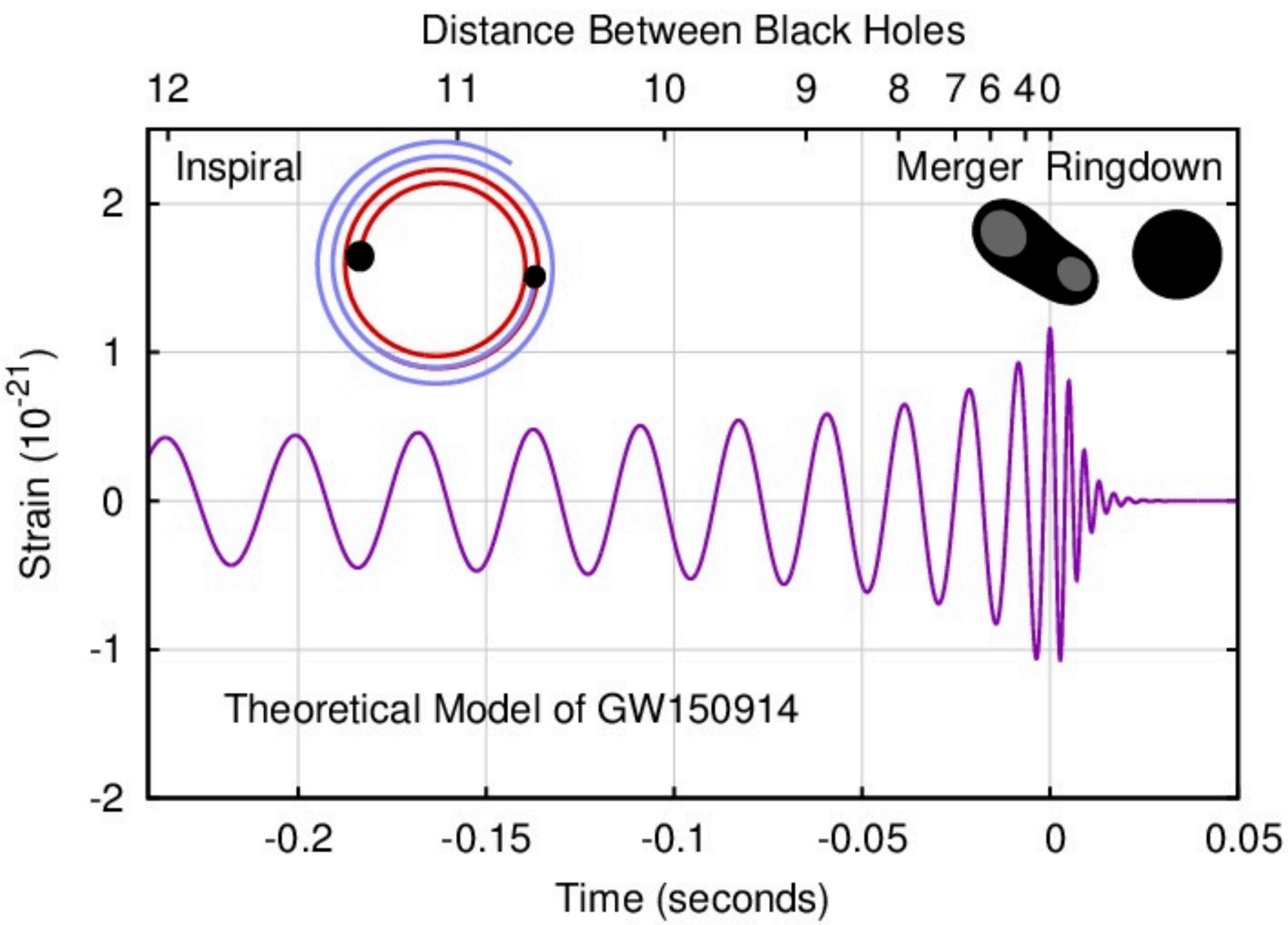

Chirp time scale

Motivation

- Newtonian dynamics of two-body inspiral problem is integrable.

- Once post-Newtonian (PN) corrections are included, the situation is not so clear, e.g., binary black holes (BBH).

- If not integrable, one would expect chaotic behavior (dense unstable orbits in phase space/resonant islands), possibly reflected in the decoherence of GW, i.e., glitches.

- If Lyapunov time scale << chirp time scale, need huge template banks for detecting GWs.

$$\delta\mathbf{X}(t) = \mathbf{L}(t)\delta\mathbf{X}(0)$$
$$\mathbf{L}(t) = \mathrm{diag}(e^{\lambda t} f(t), 0, 0, \cdots, 0)$$

$$\longrightarrow$$

$$\delta h(t) = \frac{\partial h(\mathbf{X})}{\partial \mathbf{X}} \delta\mathbf{X}(t) \simeq e^{\lambda t} g(t)$$

GW signature of EMRI

Destounis+Suvorov+Kokkota 2021

$$\eta = 10^{-6}, \quad a = 0.99M$$

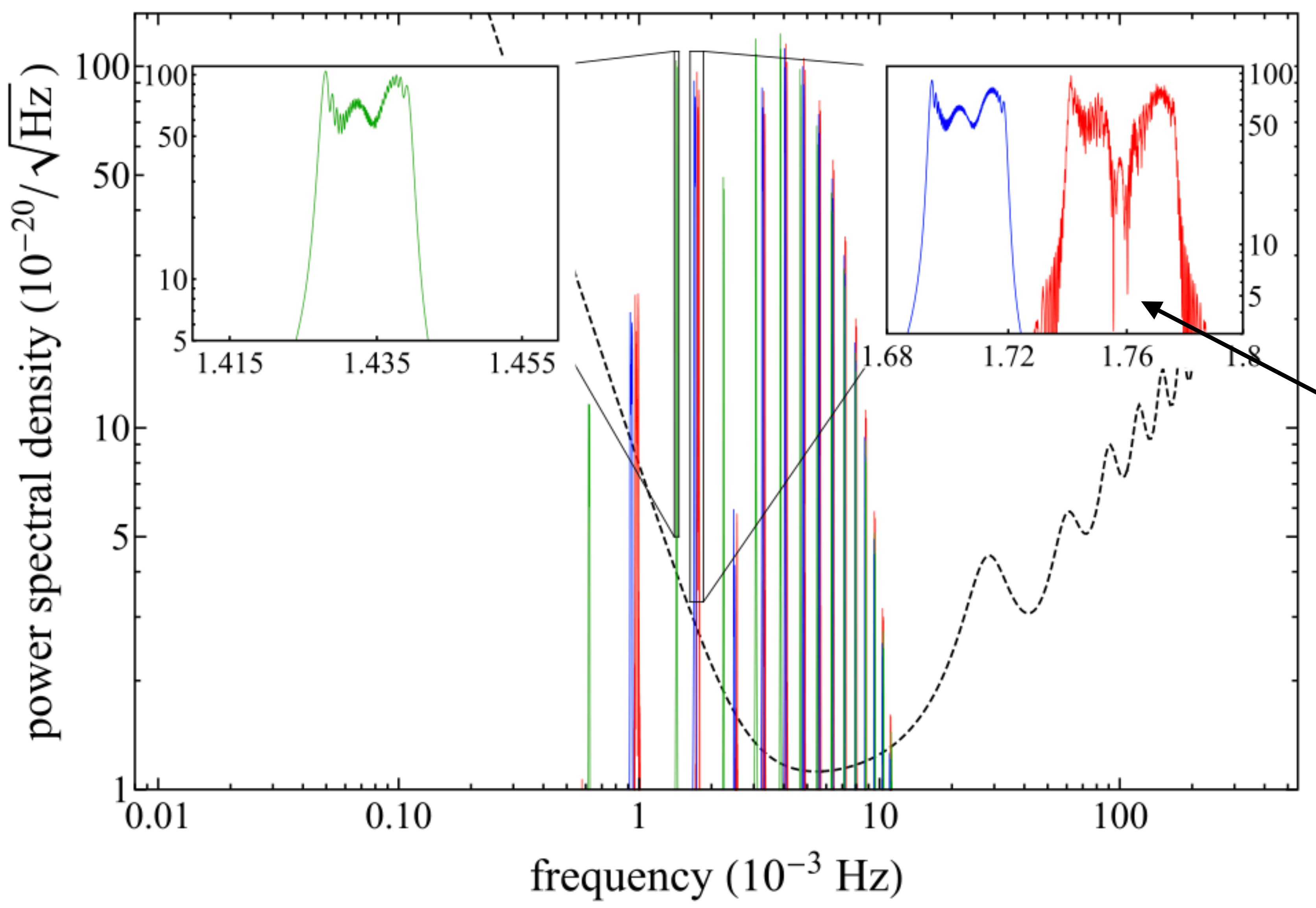

FIG. 1. Power spectral density of a Kerr (green), a non-Kerr (red), and a deformed-Kerr (blue) EMRI consisting of a light companion

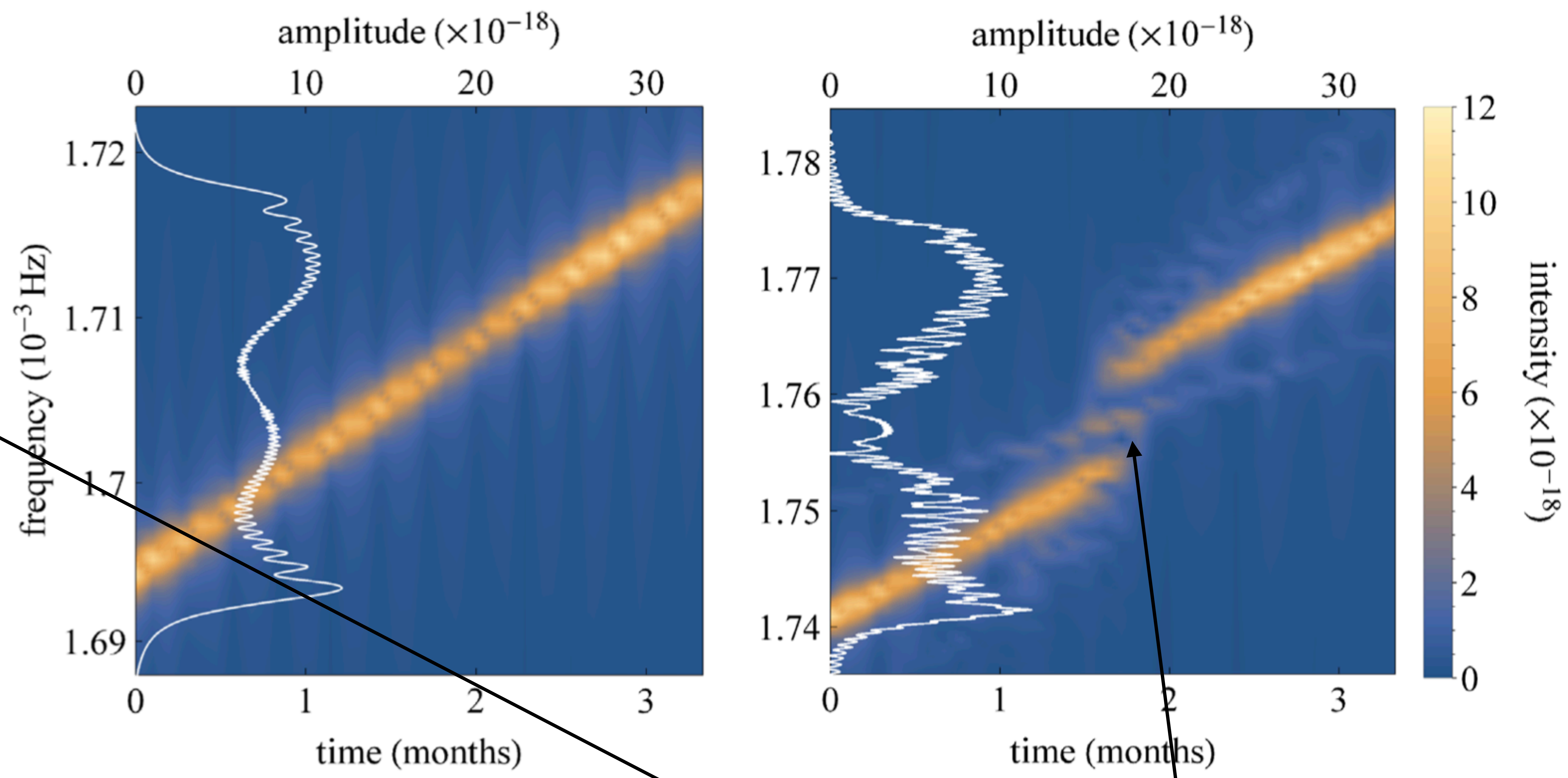

Periodogram of a deformed-Kerr (left) and a non-Kerr EMRI (right) GW, plotted below the most prominent GW peak

deformed-Kerr: intergable perturbation from Kerr metric

non-Kerr: nonintegrable perturbation from Kerr metric

GW glitch

Controversy on integraibility of PN orbits

- Debates on the (non-)integrability of inspiral dynamics of spinning binary come a long way since the year 2000. Levin 2000, Schnittman+Rasio 2001, Cornish+Levin 2002, 2003, Hartl+Buonanno 2005, Gopakumar+Konigsdorffer 2005^2, Wu+Xie 2007, Huang+Ni+Wu 2014, Wu+Huang 2015, Huang+Wu 2016
- The analytical study is technically hard to find the symplectic structure for the PN Hamiltonian. Up to 2020, some subset of 2PN is found to be integrable. Tanay+Cho+Stein 2021, Tanay+Stein+Ghersi 2021, Cho+Lee 2019, Wu+Xie 2010, Wu+Zhong 2011
- The numerical study is to calculate the Lyapunov exponents, which is computationally costly due to the complicated PN dynamics. The numerical inaccuracy is the main source of controversy.
- In this work, we find a reliable and “non-perturbative” way (i.e., EOB) to pin down the issue by finding the resonant islands.

Outline

- Effective-One-Body (EOB) dynamics
- (Non-)Integrablity
- Resonant (Birkhoff) Islands
- Our Results
- Conclusion

EOB dynamics

EOB dynamics

EOB formalism is to map PN dynamics to effective-one-body dynamics in a non-flat background. The procedure is outlined as follows:

1. Expand the PN Hamiltonian in terms of the dynamical invariants such as the reduced radial action I_R and angular momentum J.

2. Expand a probe Hamiltonian in deformed Kerr metric ansatz in a similar way.

3. Relate the probe Hamiltonian to the PN Hamiltonian to determine the metric ansatz.

4. The above mapping defines a canonical transformation between the ADM coordinates for the PN dynamics and the coordinates of the EOB metric.

- One can also choose the dynamical invariant for the unbounded orbits such as scattering angles and fits to the post-Minkowskian potential from scattering amplitudes. Damgaard+Vanhove 2021

Post-Newtonian (PN) Dynamics

- PN Hamiltonian is complicated: (2PN COM Hamiltonian of 2 non-spinning particles in ADM coord.)

$$\mathbf{q}' = \frac{\mathbf{Q}'_1 - \mathbf{Q}'_2}{GM}, \quad \mathbf{p}' = \frac{\mathbf{P}'}{\mu}, \quad \hat{H} = \frac{H}{\mu}$$

$$M = m_1 + m_2, \quad \mu = \frac{m_1 m_2}{M}, \quad \eta = \frac{\mu}{M}$$

$$\hat{H}(\mathbf{q}', \mathbf{p}') = \left(\frac{c^2}{\eta} + \frac{1}{2}\mathbf{p}'^2 - \frac{1}{q'}\right) + \frac{1}{c^2}\hat{H}_{1\mathrm{PN}}(\mathbf{q}', \mathbf{p}') + \frac{1}{c^4}\hat{H}_{2\mathrm{PN}}(\mathbf{q}', \mathbf{p}')$$

$$\hat{H}_{1\mathrm{PN}}(\mathbf{q}', \mathbf{p}') = -\frac{1}{8}(1 - 3\eta)\mathbf{p}'^4 - \frac{1}{2q'}[(3 + \eta)\mathbf{p}'^2 + \eta(\mathbf{n}' \cdot \mathbf{p}')^2] + \frac{1}{2q'^2}$$

$$\hat{H}_{2\mathrm{PN}}(\mathbf{q}', \mathbf{p}') = \frac{1}{16}(1 - 5\eta + 5\eta^2)\mathbf{p}'^6 + \frac{1}{8q'}[(5 - 20\eta - 3\eta^2)\mathbf{p}'^4 - 2\eta^2\mathbf{p}'^2(\mathbf{n}' \cdot \mathbf{p}')^2 - 3\eta^2(\mathbf{n}' \cdot \mathbf{p}')^4] + \frac{1}{2q'^2}[(5 + 8\eta)\mathbf{p}'^2 + 3\eta(\mathbf{n}' \cdot \mathbf{p}')^2] - \frac{1}{4q'^3}(1 + 3\eta)$$

- Solving the 1st principle PN dynamics is costly. This motivates to find the equivalent effective one-body (EOB) dynamics in non-flat background.

$\hat{H}(I_R, J)$

- The form of the Hamiltonian is coordinate dependent and it is hard to compare.
- One way out is to express it in terms of dynamical invariants such as I_R, J .
- Up to 2PN, the reduced radial action is $(\alpha = GM\mu)$ Buonanno+Damour 1999

$$I_R(E^{\mathrm{NR}}, J) = \alpha\sqrt{\frac{\mu}{-2E^{\mathrm{NR}}}}\left[1 + \left(\frac{15}{4} - \frac{\eta}{4}\right)\frac{E^{\mathrm{NR}}}{\mu c^2} + \left(\frac{35}{32} + \frac{15\eta}{16} + \frac{3\eta^2}{32}\right)\left(\frac{E^{\mathrm{NR}}}{\mu c^2}\right)^2\right] - J + \frac{\alpha^2}{c^2 J}\left[3 + \left(\frac{15}{2} - 3\eta\right)\frac{E^{\mathrm{NR}}}{\mu c^2}\right] + \left(\frac{35}{4} - \frac{5\eta}{2}\right)\frac{\alpha^4}{c^4 J^3}$$

- Reversely, one can obtain $(E := E^{\mathrm{NR}} + Mc^2, \quad N := I_R + J)$

$$E(N, J) = Mc^2 - \frac{\mu\alpha^2}{2N^2}\left[1 + \frac{\alpha^2}{c^2}\left(\frac{6}{NJ} - \frac{15 - \eta}{4N^2}\right) + \frac{\alpha^4}{c^4}\left(\frac{5(7 - 2\eta)}{2NJ^3} + \frac{27}{N^2J^2} - \frac{3(35 - 4\eta)}{2N^3J} + \frac{145 - 15\eta + \eta^2}{8N^4}\right)\right]$$

- This is the energy spectrum of the PN atom.
- The probe Hamiltonian in the EOB metric can be expressed in a similar form.

EOB Map

relative boost factor: $\gamma = \frac{p_1 \cdot p_2}{m_1 m_2} = \frac{E^2 - m_1^2 - m_2^2}{2m_1 m_2} \longrightarrow E = M\sqrt{1+2\nu(\gamma-1)}$

The energy of the reduced test-body: $E_{\rm eff} = \gamma\mu \longrightarrow E = M\sqrt{1+\frac{2\eta}{\mu}(E_{\rm eff}-1)}$

Test-body dynamics: $g^{\mu\nu}_{\rm eff}(\mathbf{q})p_\mu p_\nu + \mu^2 c^2 = 0 \qquad \text{with} \qquad E_{\rm eff} = -p_0$

$$ds^2_{\rm eff} = -A(r)dt^2 + B(r)dr^2 + r^2 d\Omega^2 \qquad A(r) = 1 + \frac{a_1}{c^2 r} + \frac{a_2}{c^4 r^2} + \frac{a_3}{c^6 r^3} + \cdots, \qquad B(r) = 1 + \frac{b_1}{c^2 r} + \frac{b_2}{c^4 r^2} + \cdots$$

$$\longrightarrow \qquad \hat{H}_{\rm eff} = c^2\sqrt{A(r)\Big[1 + \frac{\mathbf{p}'^2}{c^2} + \frac{(\mathbf{n}'\cdot\mathbf{p}')^2}{c^2}\big(\frac{1}{B(r)} - 1\big)\Big]}$$

Task: **Fix** a_i, b_i **by matching** $\hat{H}(\mathbf{q}', \mathbf{p}')$ **to** $\hat{H}_{EOB}(\mathbf{q},\mathbf{p}) = M\sqrt{1+\frac{2\eta}{\mu}\Big(\hat{H}_{\rm eff}(\mathbf{q},\mathbf{p}) - \mu\Big)}$

in the space of dynamical invariants, i.e., I_R, J**.**

$$\longrightarrow \qquad a_1 = -2,\ a_2 = 0,\ a_3 = 2\eta,\ b_1 = 2,\ b_2 = 4 - 6\eta$$

and

$$p'_i dq'^i + q^i dp^i = dG(q', p)$$

$$G(q', p) = q'^i p_i + \frac{1}{c^2}G_{\rm 1PN}(q', p) + \frac{1}{c^4}G_{\rm 2PN}(q', p)$$

Including spins and Higher PN

- However, if the EOB metric still preserves the symmetrical symmetry, then the geodesic motion is planar and cannot be chaotic.

- Once the component spins $\mathbf{S}_{1,2}$ are turned on, $H_{\rm eff} = H^{NS} + H^{S}$ Damour 2001, Barausse+Buonanno 2010, 2011

$$H^{NS}(\mathbf{S}_{\rm Kerr}, \cancel{\mathbf{S}^*}) = \beta^i p_i + \alpha\sqrt{m^2 + \gamma^{ij}p_i p_j + Q_{3PN\uparrow}(p)}, \qquad \alpha := 1/\sqrt{-g^{tt}_{\rm eff}}, \quad \beta^i := g^{ti}_{\rm eff}/g^{tt}_{\rm eff}, \quad \gamma^{ij} := g^{ij}_{\rm eff} - g^{ti}_{\rm eff}g^{tj}_{\rm eff}/g^{tt}_{\rm eff}$$

$$H^{S}(\mathbf{S}_{\rm Kerr}, \mathbf{S}^*) = H^{S}_{SO,1.5PN} + H^{S}_{SO,2.5PN} + H^{S}_{SS,2PN}, \quad H^{S}_{SO,1.5/2.5PN} \sim \mathcal{O}(\mathbf{S}^*), \quad H^{S}_{SS,2PN} \sim \mathcal{O}(\mathbf{S}^{*2})$$

$$\mathbf{S}_{\rm Kerr} = \sigma + \frac{1}{c^2}\mathbf{\Delta}, \quad \mathbf{S}^* = \sigma^* + \frac{1}{c^2}\Delta_{\sigma^*}, \quad \sigma = \mathbf{S}_1 + \mathbf{S}_2, \quad \sigma^* = \frac{m_2}{m_1}\mathbf{S}_1 + \frac{m1}{m_2}\mathbf{S}_2,$$

$$\mathbf{\Delta}_\sigma = -\frac{1}{16}\left\{12\mathbf{\Delta}_{\sigma^*} + \eta\left[\frac{2M}{r}(4\sigma - 7\sigma^*) + 6(\hat{\mathbf{p}}\cdot\hat{\mathbf{n}})^2(6\sigma + 5\sigma^*) - \hat{\mathbf{p}}^2(3\sigma + 4\sigma^*)\right]\right\}$$ but $\mathbf{\Delta}_{\sigma^*}$ is an arbitrary function as long as it is $\mathcal{O}(\eta)$ as $\eta \to 0$.

- For simplicity, we will turn off $\mathbf{S}^*$ by choosing the appropriate $\mathbf{\Delta}_{\sigma^*}$. It is also automatically ensured by MPD equation $\frac{DS^{\mu\nu}}{d\tau} = P^\mu u^\nu - P^\mu u^\nu \sim \mathcal{O}((\mathbf{S}^*)^2)$. Thus, $H^S = 0$.

- We also restrict to 2PN so that $Q_{3PN\uparrow}(p) = 0$ so that the resultant EOB dynamics will be "a non-spinning particle of mass μ moving in a deformed Kerr background". As we will see the geodesic dynamics is non-integrable.

2PN EOB metric: deformed Kerr

$$ds^2_{\text{eff}} = g_{tt}dt^2 + g_{rr}dr^2 + g_{yy}dy^2 + g_{\phi\phi}d\phi^2 + 2g_{t\phi}dtd\phi.$$

$$g^{tt} = -\frac{\Lambda_t}{\Delta_t \Sigma}, \qquad g^{t\phi} = -\frac{\tilde{\omega}_{fd}}{\Delta_t \Sigma}, \qquad g^{rr} = \frac{\Delta_r}{\Sigma},$$

$$g^{yy} = \frac{1-y^2}{\Sigma}, \qquad g^{\phi\phi} = \frac{1}{\Lambda_t}\left(-\frac{\tilde{\omega}_{fd}^2}{\Delta_t \Sigma} + \frac{\Sigma}{1-y^2}\right),$$

$$g^{tt} = -\frac{g_{\phi\phi}}{g_{t\phi}^2 - g_{tt}g_{\phi\phi}}, \qquad g^{t\phi} = \frac{g_{t\phi}}{g_{t\phi}^2 - g_{tt}g_{\phi\phi}},$$

$$g^{\phi\phi} = -\frac{g_{tt}}{g_{t\phi}^2 - g_{tt}g_{\phi\phi}}, \qquad g^{rr} = \frac{1}{g_{rr}}, \qquad g^{yy} = \frac{1}{g_{yy}}.$$

$$\Sigma = r^2 + a^2y^2, \qquad \Delta = r^2 - 2Mr + a^2, \qquad X = r^2 + a^2,$$

$$\Delta_t = \Delta + \eta F(r), \qquad \Delta_r = \Delta_t[1 + \eta G(r)],$$

$$\tilde{\omega}_{fd} = a(X - \Delta)[1 + \eta H(r)],$$

$$\Lambda_t = X^2 - a^2\Delta_t(1 - y^2),$$

$$F(r) = \frac{2M^3}{r},$$

$$G(r) = \frac{1}{\eta}\ln\left[1 + 6\eta\frac{M^2}{r^2}\right],$$

$$H(r) = \frac{1}{2r^2}(\omega_1^{fd}M^2 + \omega_2^{fd}a^2).$$

$$a := \frac{|\mathbf{S}_1 + \mathbf{S}_2|}{M},$$

1. Kerr bound $|S_i| \leq m_i^2$ **implies** $a \leq (1-2\eta)M < a_{\text{ext}}(\eta)$.

2. As $\hat{H}_{EOB}(\mathbf{q},\mathbf{p}) = M\sqrt{1 + \frac{2\eta}{\mu}\left(\hat{H}_{\text{eff}}(\mathbf{q},\mathbf{p}) - \mu\right)}$,

the geodesic dynamics for H_{eff} **and** H_{EOB} **are equivalent up to a time rescaling.**

3. We just consider geodesic dynamics for $\hat{H}_{\text{eff}}$ **by setting** $\mu = 1$**, and the energy** E **and azimuthal angular momenta** L_z **are conserved.**

4. The reduced Hamiltonian constraint:

$$\dot{r}^2 + \frac{g^{rr}}{g^{yy}}\dot{y}^2 + V_{\text{eff}} = 0,$$

non-separable!

$$V_{\text{eff}} = g^{rr}(1 + g^{tt}E^2 + g^{\phi\phi}L_z^2 - 2g^{t\phi}EL_z).$$

(Non-)Integrability

(Non-)Integrable orbits

- A dynamical system is integrable: # of conserved charges = # of d.o.f.
- Non-spinning particle moving in Kerr black hole is integrable: 4 conserved charges = mass, E, L_z, and Carter constant C $\longrightarrow$ The Hamiltonian constraint is separable.
- The generator for C is a Killing tensor or Killing-Yano tensor of rank 2.
- For Boyer-Lindquist type coord (r, x, ϕ, t): Papadopoulos+Kokkota 2018

If

$$g^{ab} = \frac{1}{A_1(r)+B_1(x)} \begin{pmatrix} A_2(r) & 0 & 0 & 0 \\ 0 & B_2(x) & 0 & 0 \\ 0 & 0 & A_3(r)+B_3(x) & A_4(r)+B_4(x) \\ 0 & 0 & A_4(r)+B_4(x) & A_5(r)+B_5(x) \end{pmatrix}$$

$$A_i(r), \quad B_i(x)$$

A nontrivial rank 2 Killing tensor

$$K^{ab} = \frac{1}{A_1(r)+B_1(x)} \begin{pmatrix} A_2(r)B_1(x) & 0 & 0 & 0 \\ 0 & -B_2(x)A_1(r) & 0 & 0 \\ 0 & 0 & B_1(x)A_3(r)-A_1(r)B_3(x) & B_1(x)A_4(r)-A_1(r)B_4(x) \\ 0 & 0 & B_1(x)A_4(r)-A_1(r)B_4(x) & B_1(x)A_5(r)-A_1(r)B_5(x) \end{pmatrix}$$

Apply PK to 2PN EOB

- Apply PK criterion to the 2PN EOB metric, we have

$$A_1(r) = r^2, \quad B_1(y) = a^2 y^2, \quad A_2(r) = \Delta_r, \quad B_2(y) = 1 - y^2, \quad A_5(r) = -\frac{X^2}{\Delta_t}, \quad B_5(y) = a^2\left(1 - y^2\right),$$

$$A_4(r) = -\frac{a\,(X-\Delta)\left[1 + \eta H(r)\right] + \Delta_t}{\Delta_t}, \quad B_4(y) = 1$$

$$A_3(r) + B_3(y) = \frac{1}{1-y^2} - \frac{a^2}{\Delta_t} - \frac{\eta a^2\Big(X - \Delta_t + (X-\Delta)[1+\eta H(r)]\Big)\Big((X-\Delta)H(r) + F(r)\Big)}{\Delta_t\Big[X^2 - a^2\Delta_t(1-y^2)\Big]}$$

- PK fails by the last term $\sim \mathcal{O}(\eta a^2)$. It implies no rank 2 Killing tensor exists, and the dynamics is non-integrable if there exists no higher rank Killing tensor.

Resonant Islands

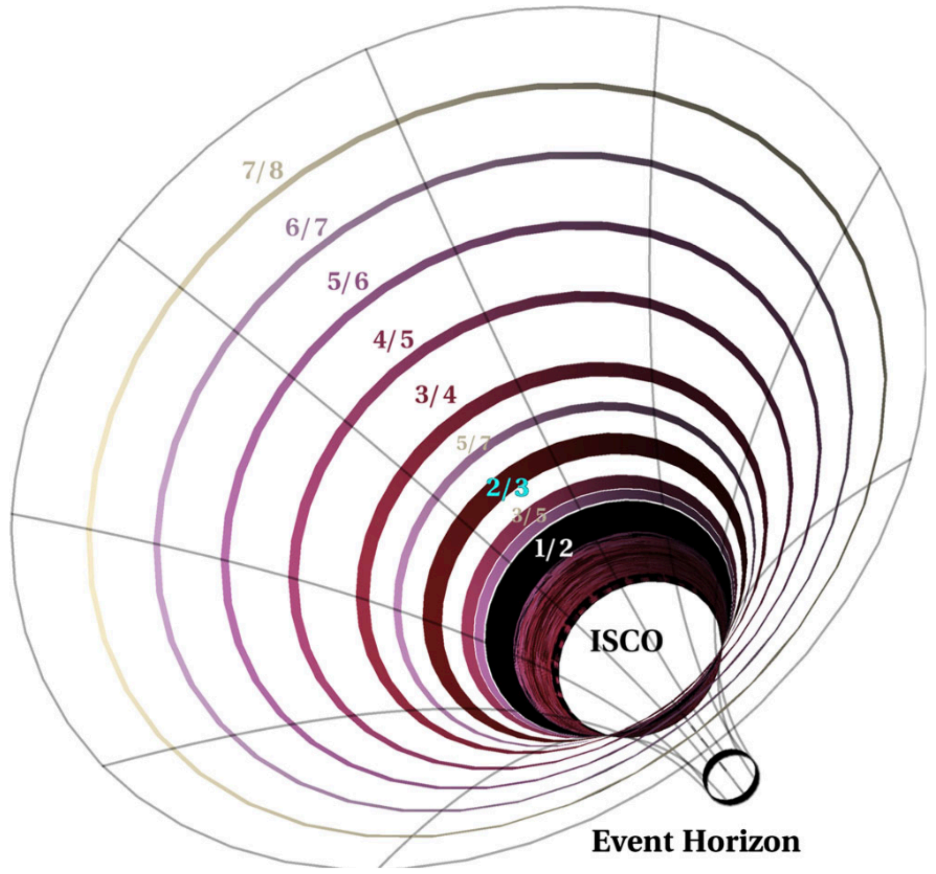

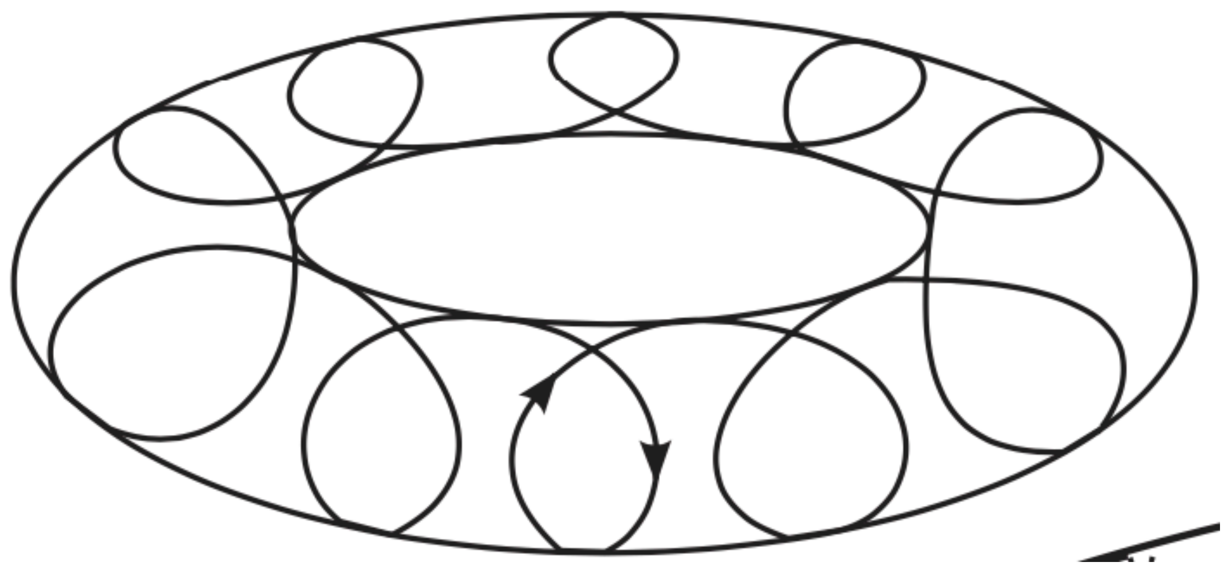

Resonant Orbits

Brink+Geyer+Hinderer 2015

- For a bound Kerr orbit: $(\frac{dr}{d\tau_M})^2 + V_r(r) = 0, \quad (\frac{dy}{d\tau_M})^2 + V_y(y) = 0.$ The orbits oscillate between the turning points in both r and y directions with frequency ω_r and ω_y, respectively.
- The orbits can be visualized as trajectories on a torus with its size determined by E, L_z and C. If ω_r/ω_y is irrational enough, the orbit will cover the torus densely, i.e., KAM tori.
- Otherwise, the orbits are called resonant orbits. These orbits are unstable when subjected to non-integrable perturbations.
- KAM theorem: The KAM tori will be smoothly deformed provided ω_r/ω_y is irrational enough and the perturbation is weak. This implies that the resonant orbits could be destroyed.

Poincare (surface of) section

- One way to characterize the chaotic behavior is the Poincare section/map of the phase space, invariant curves on the $(r, \dot{r})$ plane with $\dot{y} > 0$.

- The invariant curves are continuous closed curves for the Kerr orbits, i.e., the periodic motion is a discrete map on an invariant curve.

- For the non-Kerr orbits, there exist Birkhoff (chains of) islands around the resonant Kerr orbits.

Apostolatos+Lukes-Gerakopoulos+Contopoulos 2009, 2011

Destounis+Suvorov+Kokkotas 2020

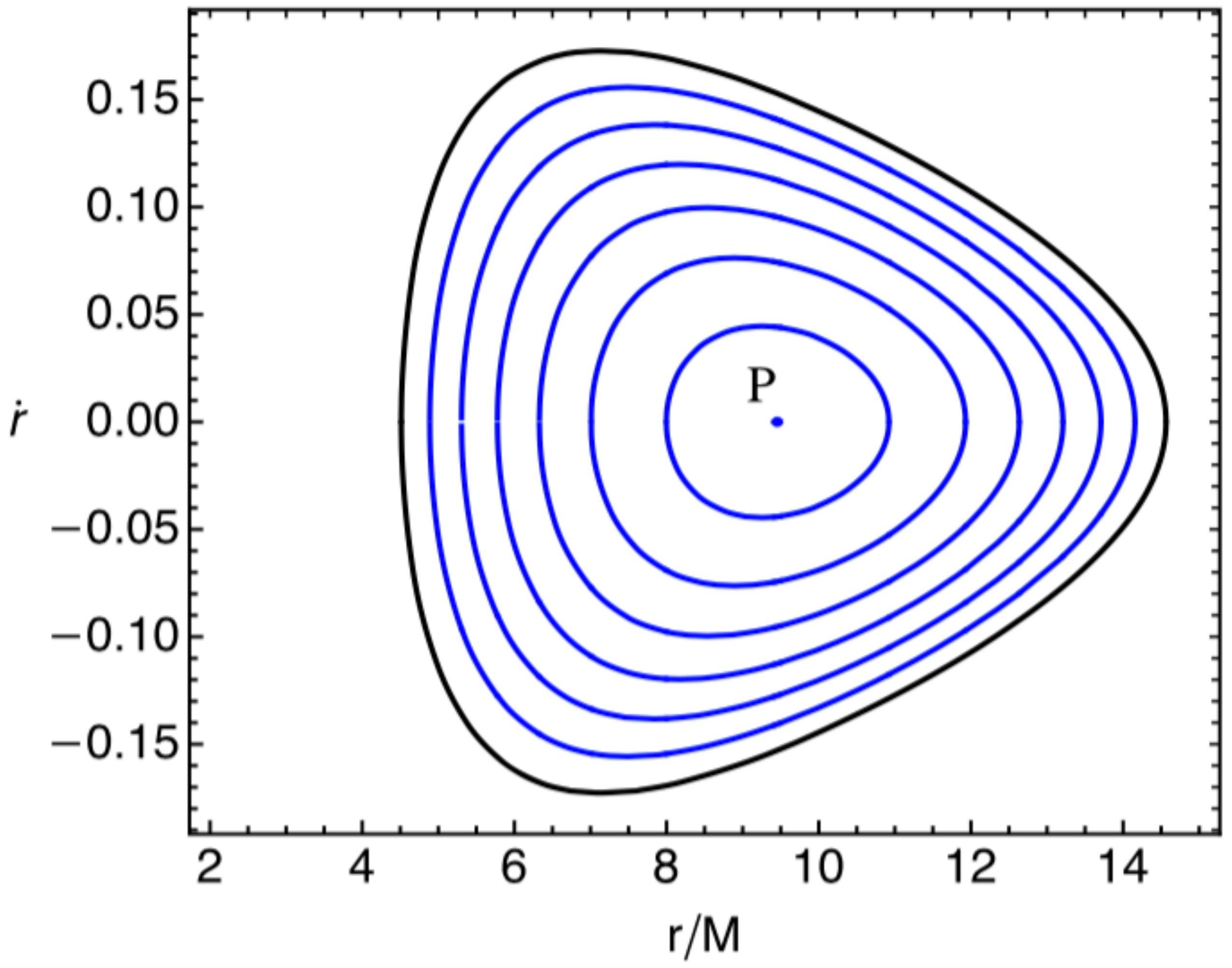

Kerr

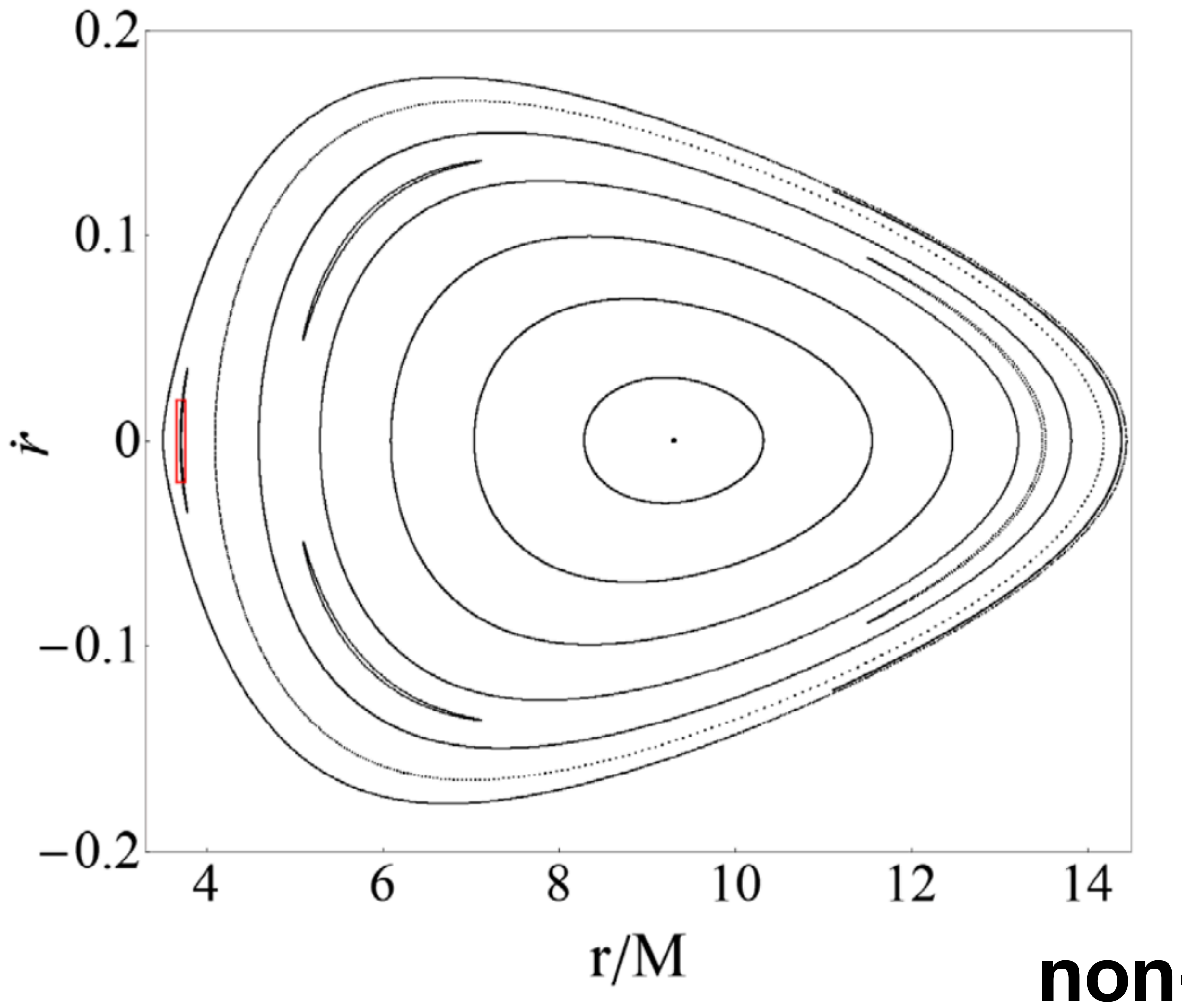

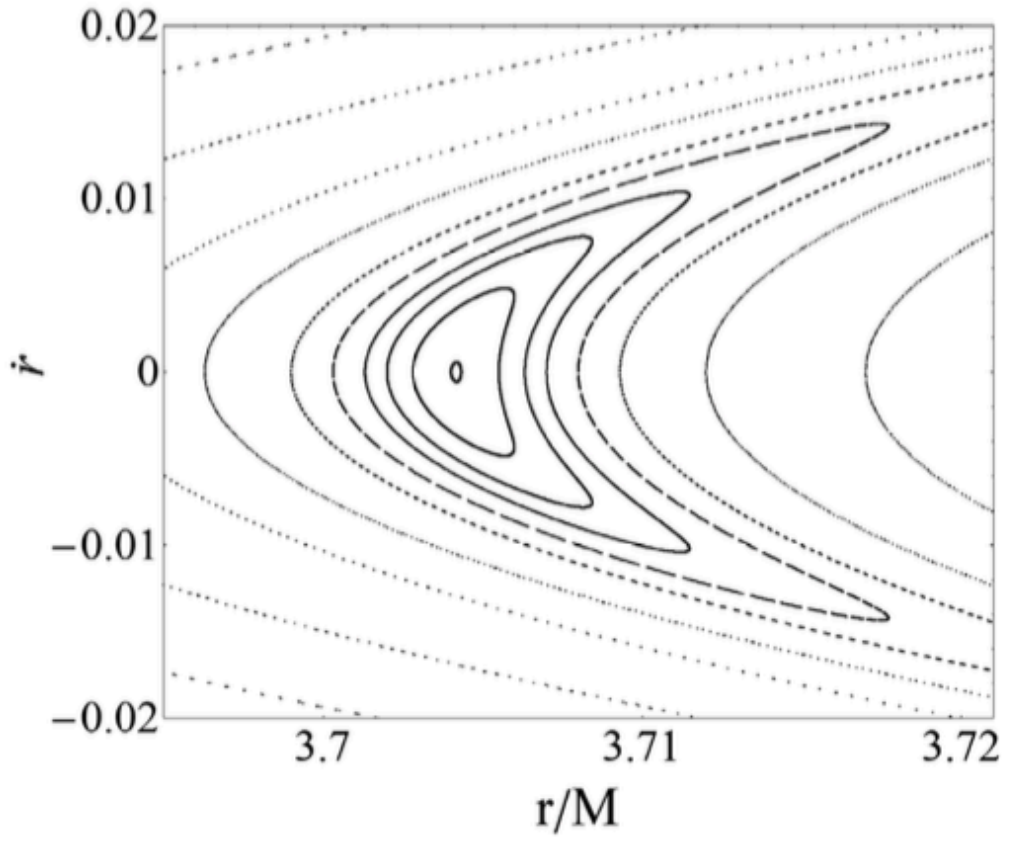

non-Kerr

Rotation Curve

- One can characterize the Birkhoff islands by tracing the piercings on the Poincare section. Precisely, define the rotation number as follows: $\nu_\theta = \lim_{N\to\infty} \frac{1}{2\pi N} \sum_{i=1}^{N} \vartheta_i$ where ϑ_i = the angle between the position vectors of the i-th and $(i+1)$-th piercings of a given orbit on the Poincare section.
- Scanning ν_θ along the r-axis ($y = \text{const}.$), we can construct the rotation curve $\nu_\theta(r)$.
- The rotation curve is continuous for Kerr orbits, but shows plateaux at low rational values.

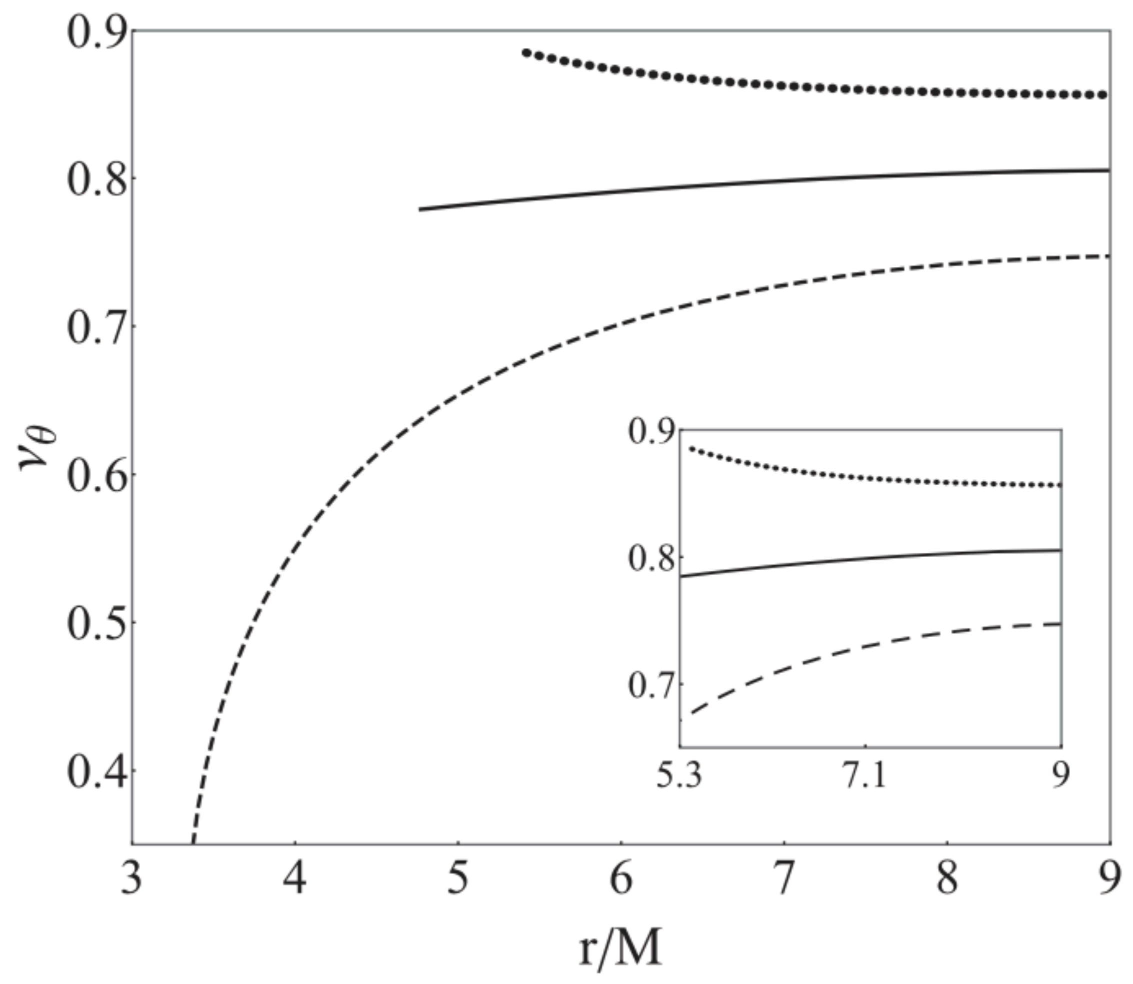

Kerr

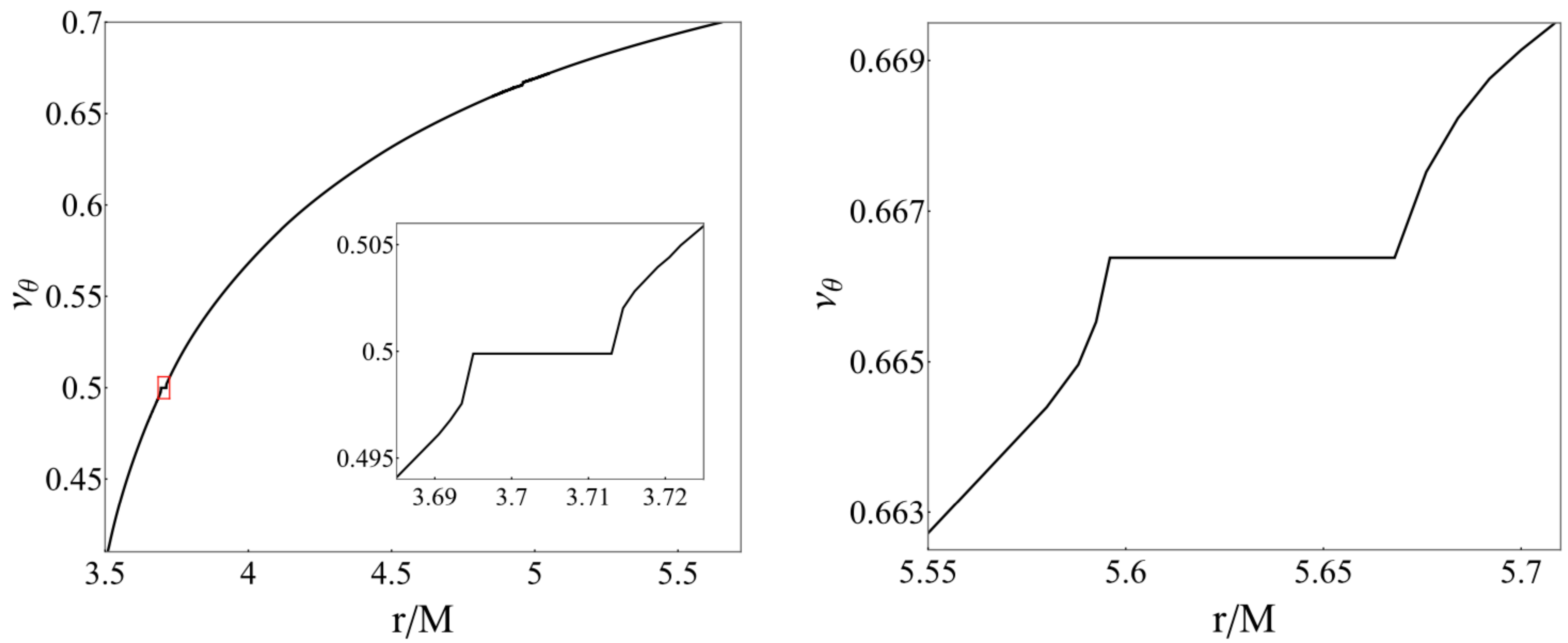

non-Kerr

Destounis+Suvorov+Kokkotas 2020

Our Results

Chaos of EOB dynamics

- From PK test, we see that the EOB dynamics can be non-integrable, thus yields non-Kerr orbits. We verify this is indeed the case.

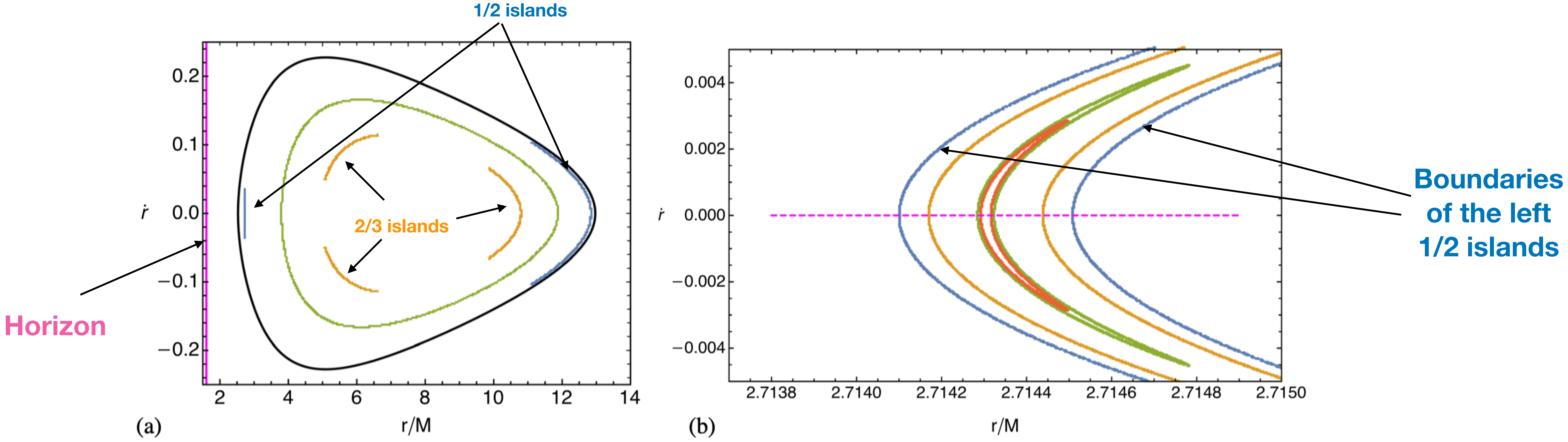

FIG. 3. Poincaré surface of section for geodesic motions in the EOB metric (16) for the spin parameter $a = 0.67\ M$, symmetric mass ratio $\eta = 0.15$, energy $E = 0.942$, and azimuthal angular momentum $L_z = 2.76\ M$. (a) Birkhoff islands (blue, 1/2 resonance; orange, 2/3 resonance) and one KAM curve (green). The vertical magenta line indicates the event horizon. (b) Enlargement of the left branch of the 1/2-resonant islands.

Rotation Curve

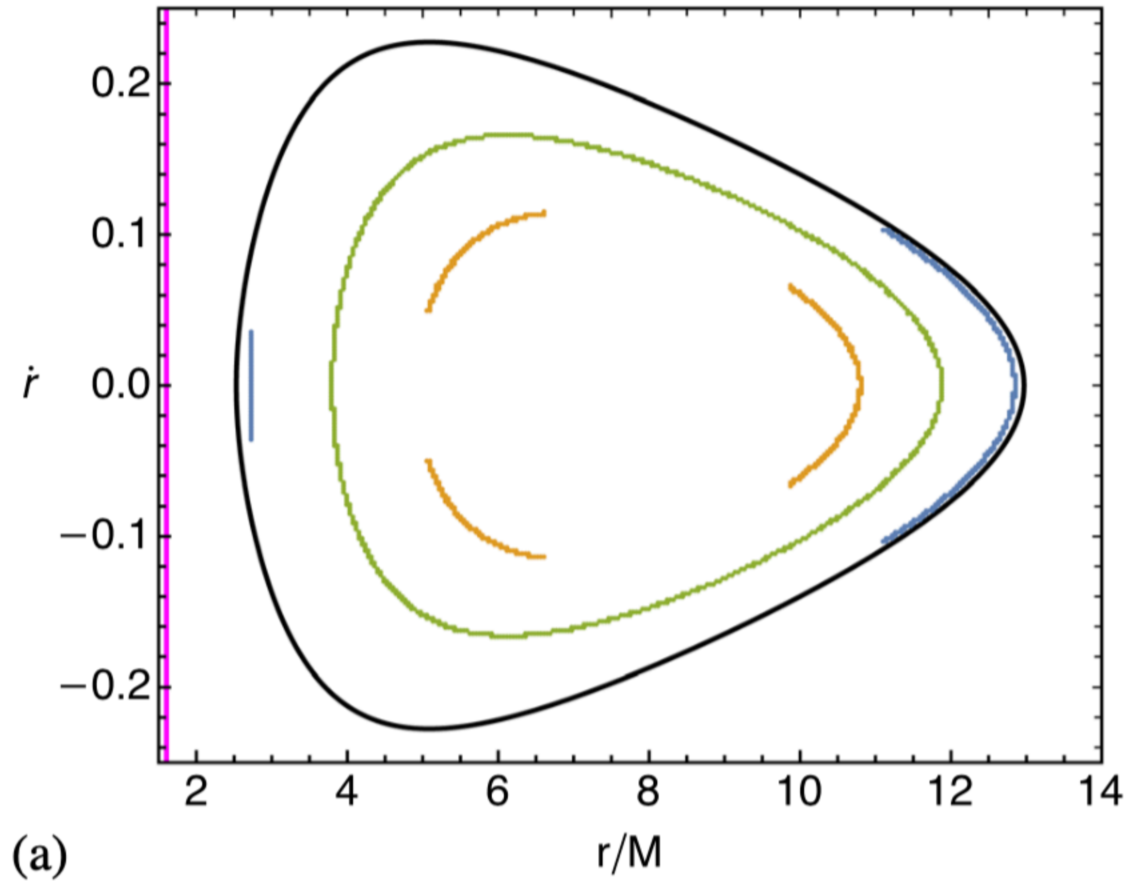

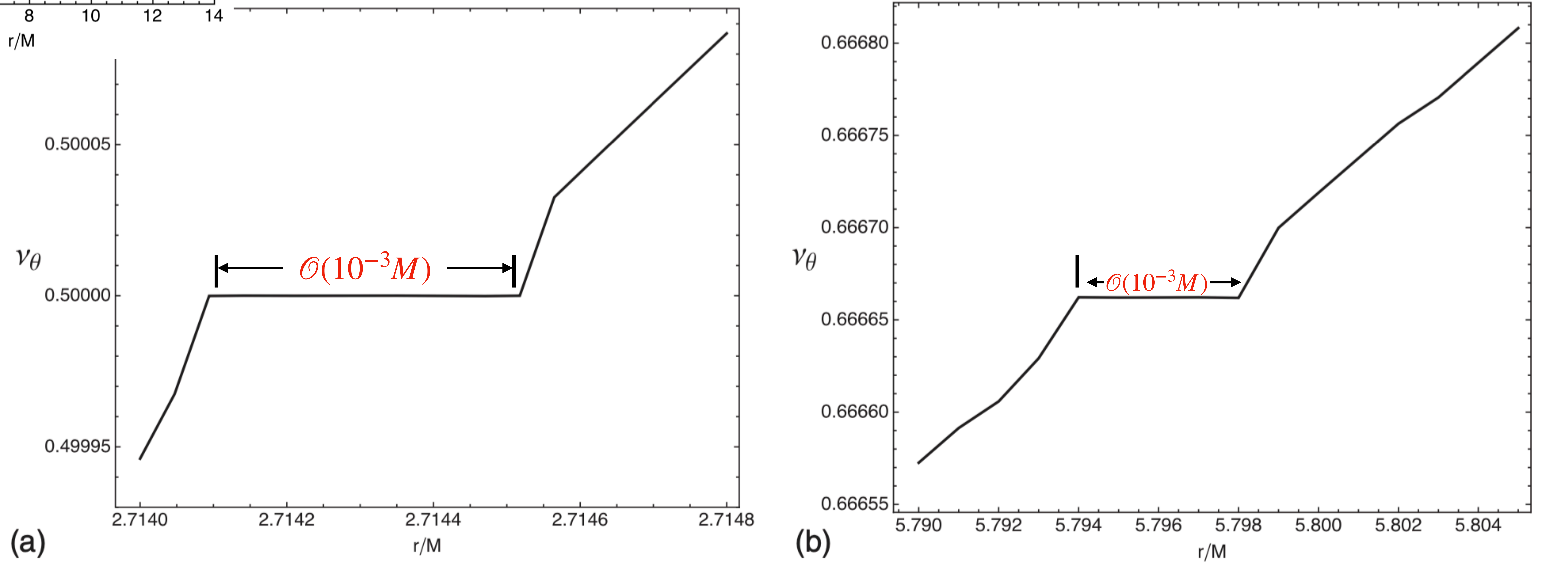

FIG. 4. (a) The rotation curve drawn along the magenta dashed line in Fig. 3(b). The plateau has a constant rotation number $\nu_\theta = 1/2$ and corresponds to the $1/2$-resonant Birkhoff islands shown in Fig. 3. (b) The rotation curve drawn along a horizontal line in Fig. 3(a) that crosses the upper-left branch of the $2/3$-resonant islands. The plateau appears as shown in both cases because the rotation number remains a constant when crossing an island.

$$a > a_{\text{ext}}(\eta) > (1 - 2\eta)M$$

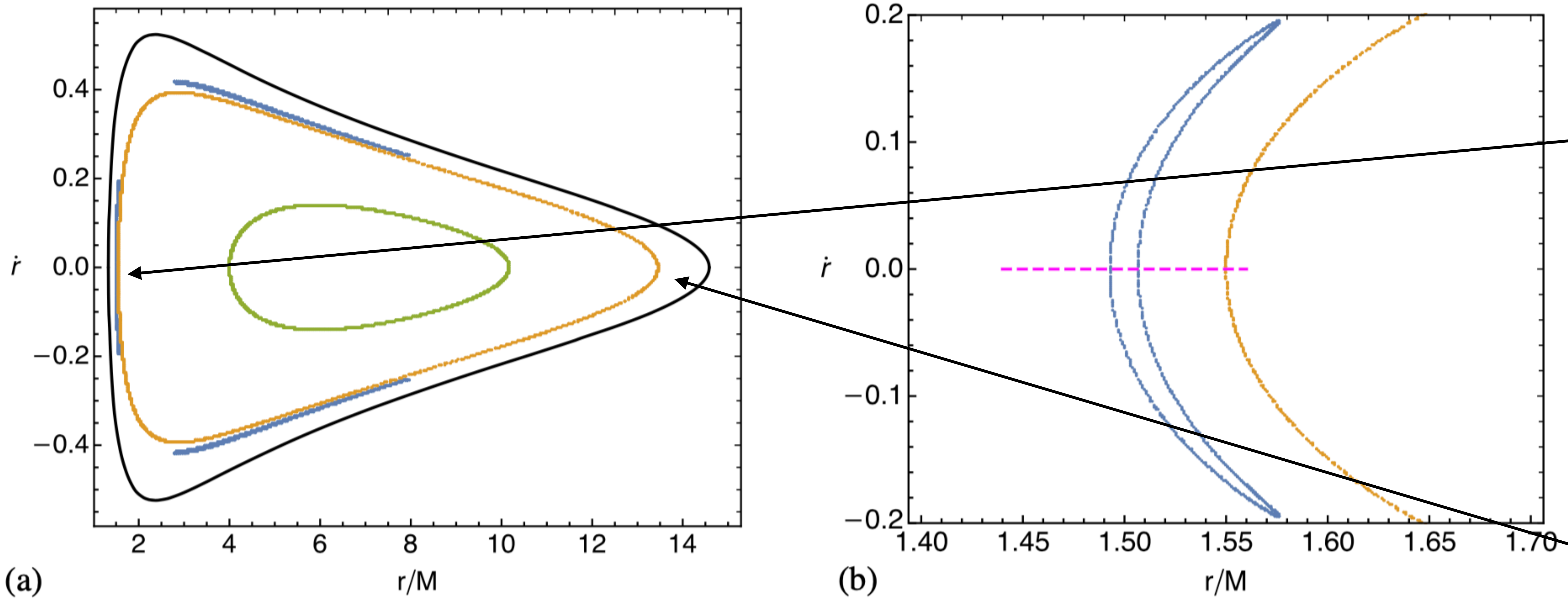

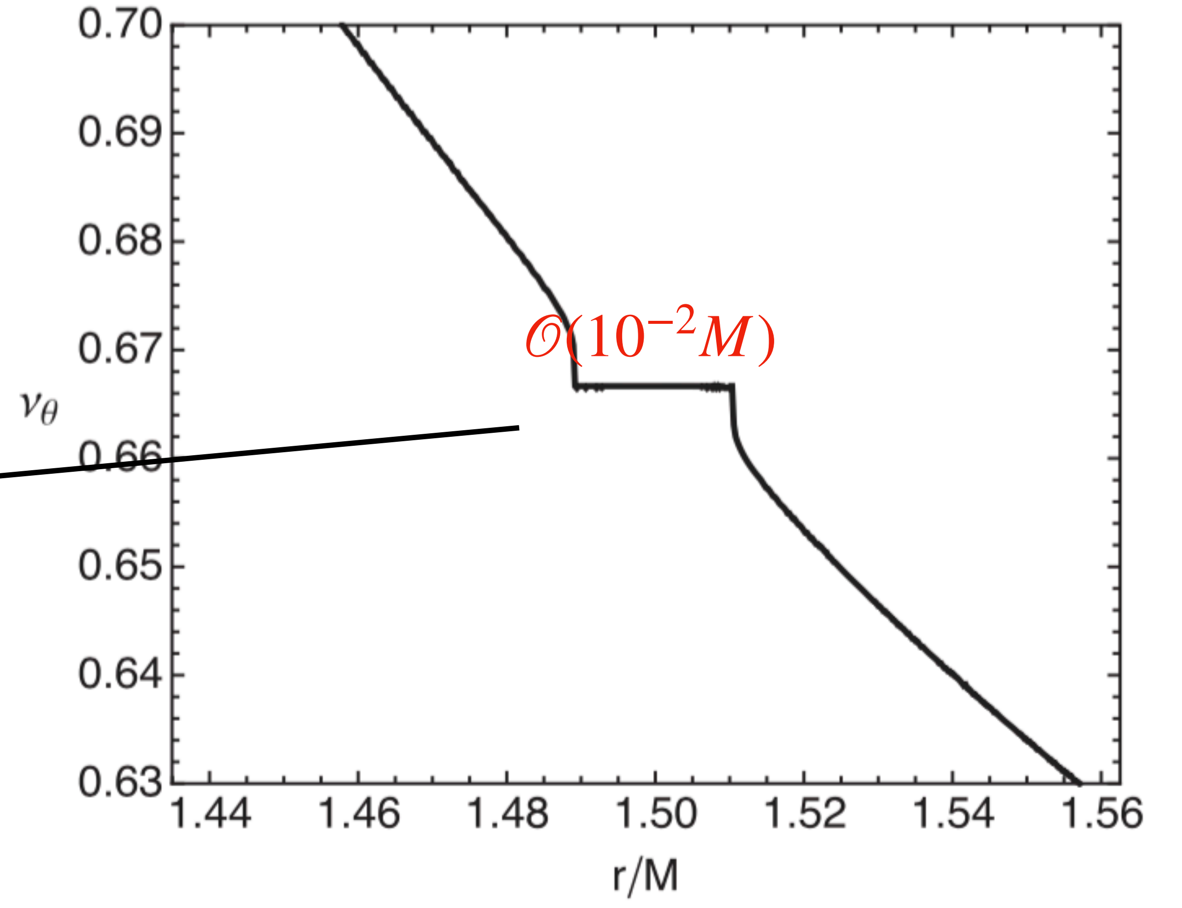

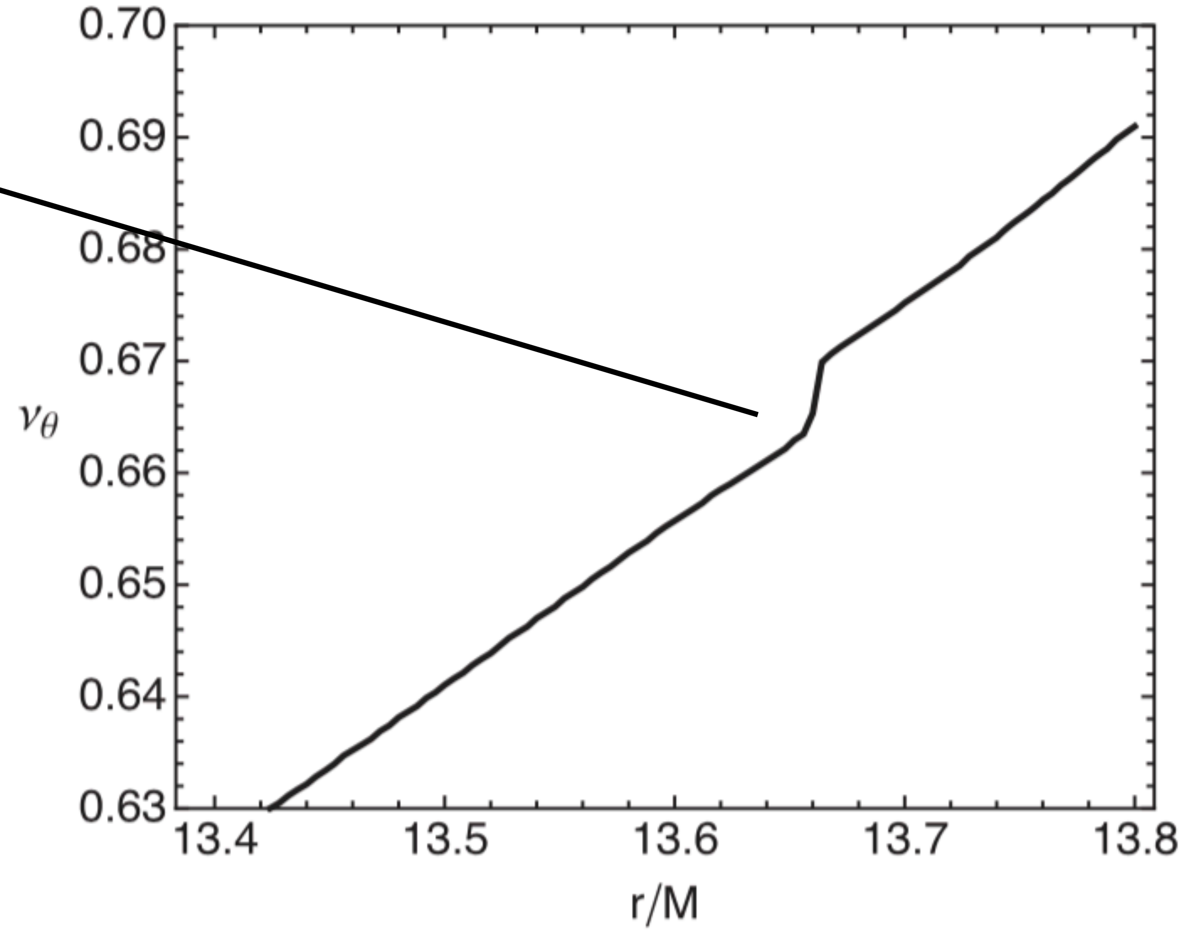

FIG. 5. Poincaré surface of section for geodesic motions in the EOB metric (16) for the spin parameter $a = 0.92\ M$, symmetric mass ratio $\eta = 0.15$, energy $E = 0.9367$, and azimuthal angular momentum $L_z = 1.7542\ M$. (a) KAM curves and Birkhoff islands (2/3 resonance) for initial conditions $(r_0, y_0, \dot{r}_0) = (1.493\ M, 0.1, 0)$ (blue), $(1.55\ M, 0, 0)$ (orange), and $(4\ M, 0, 0)$ (green). (b) Enlargement of the 2/3-resonant Birkhoff island (blue) with initial condition $(r_0, y_0, \dot{r}_0) = (1.493\ M, 0.1, 0)$. A nearby KAM curve is also shown (orange).

Birkhoff Islands

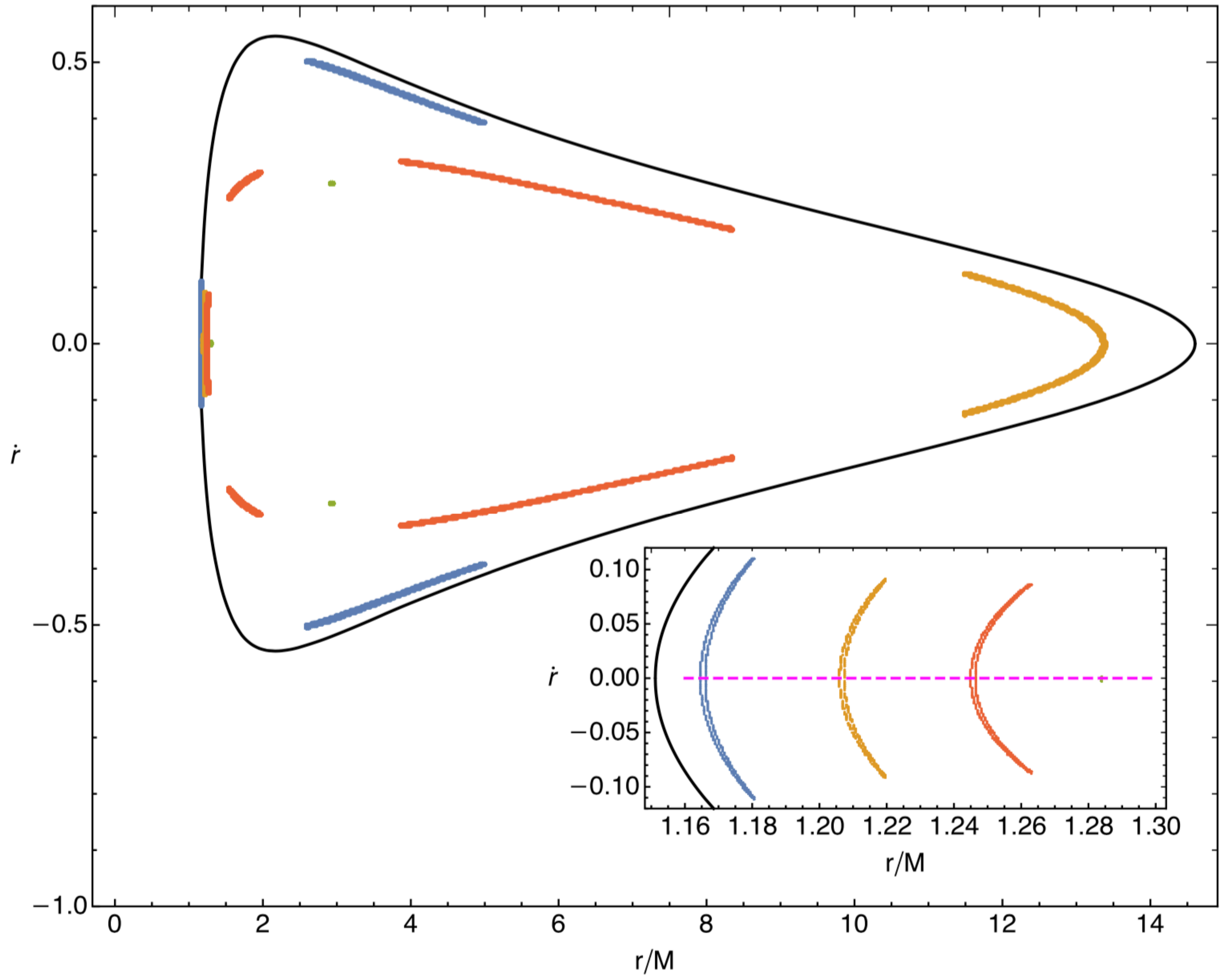

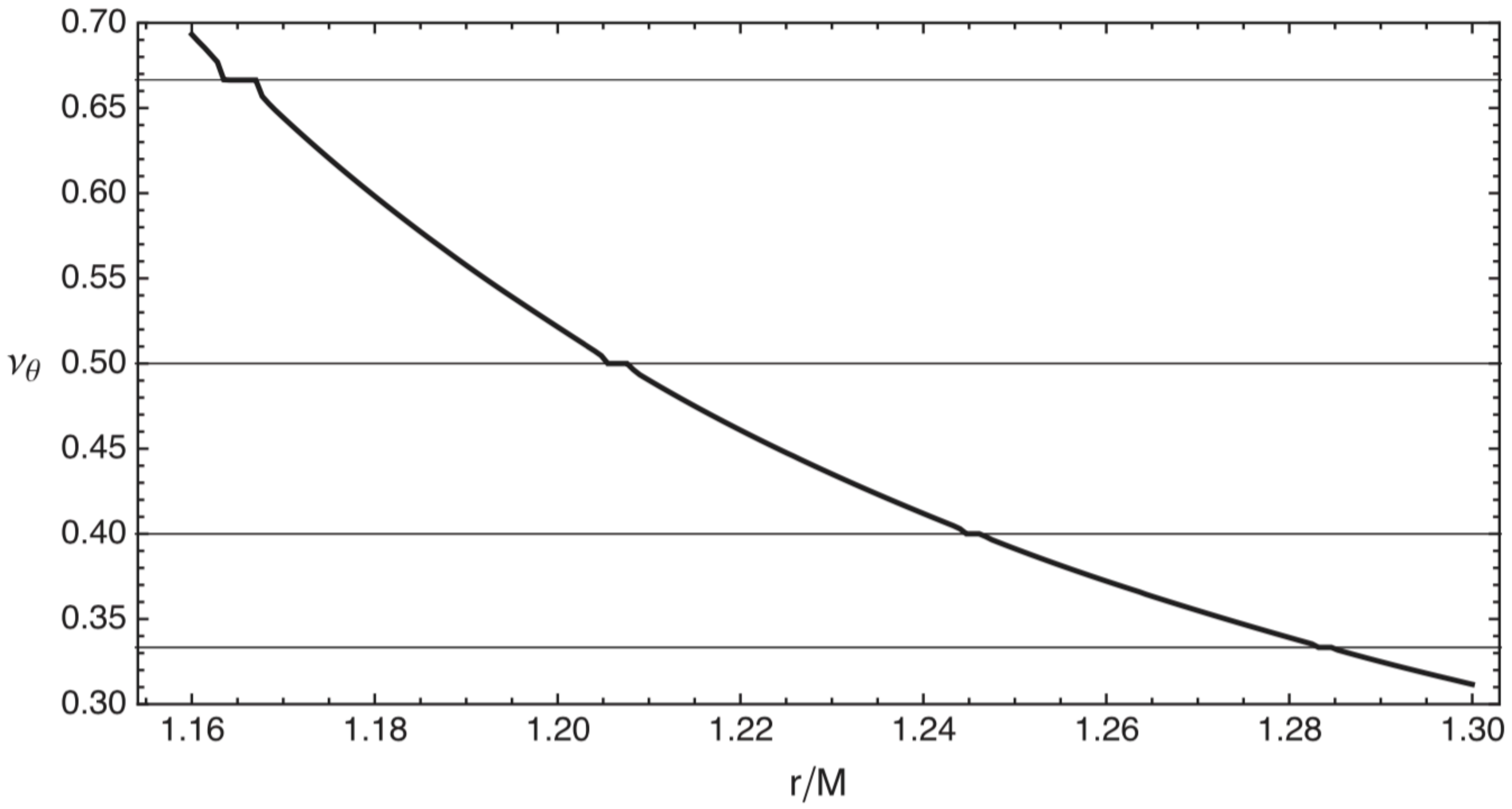

FIG. 8. Birkhoff chains of islands for 2PN Hamiltonian for $\eta = 0.15$ and $a = 0.86\ M$. Inset: Enlargement of the islands on the left edge of the Poincaré surface of section, which consists of 2/3 (blue), 1/2 (orange), 2/5 (red), and 1/3 resonances (green).

Strength of Chaos

- As seen that the PK breaking terms $\sim \mathcal{O}(\eta a^2)$, here shows some cases for $a_{\rm crit}(\eta)$ below which the plateau is too thin ($< 10^{-3}M$).

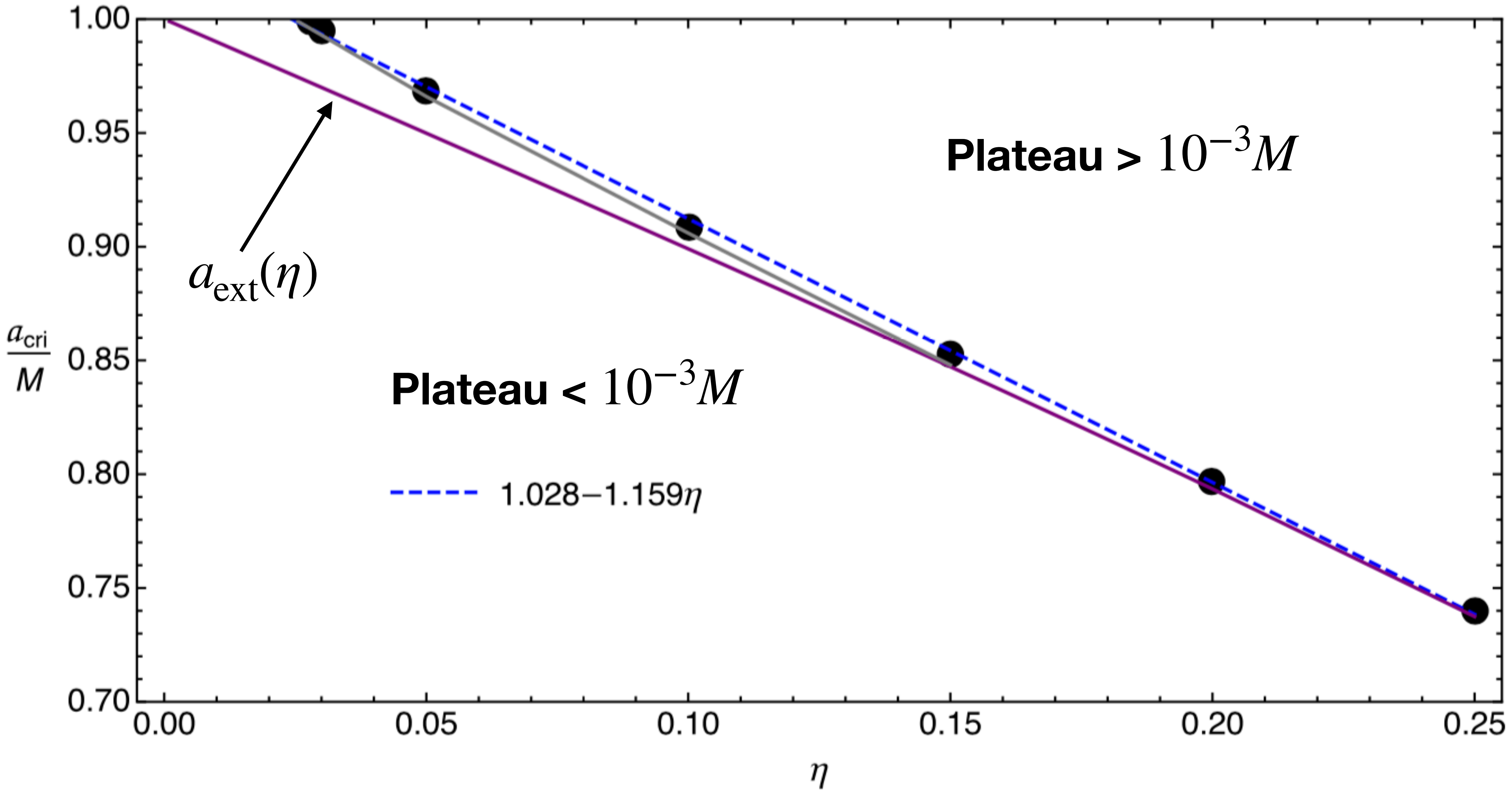

FIG. 10. The critical spin $a_{\rm cri}$ for some values of the symmetric mass ratio η (black points) upon fixing $E = 0.9367$ and $L_z = 1.7542\ M$. The points fit very well with a linear function (blue dashed line). Below the blue dashed line or the gray curve, the leftmost 2/3-resonant island either disappears or becomes too small to measure. Also, the extremality bound $a_{\rm ext}(\eta)$ is shown by the purple curve. Note that $a_{\rm cri}$ as a function of η depends also on the choice of E and L_z. We can also observe that the case with closed CZV

Preliminary 3PN result

$$F_{3PN}(r) = \frac{2M^3}{r} + \frac{M^4}{r^2}\left(\frac{94}{3} - \frac{41}{32}\pi^2\right),$$

$$G_{3PN}(r) = \frac{1}{\eta}\ln\left[1 + 6\eta\frac{M^2}{r^2} + 2(26-3\eta)\eta\frac{M^3}{r^3}\right].$$

however, $Q_{3PN}(p) = 0.$

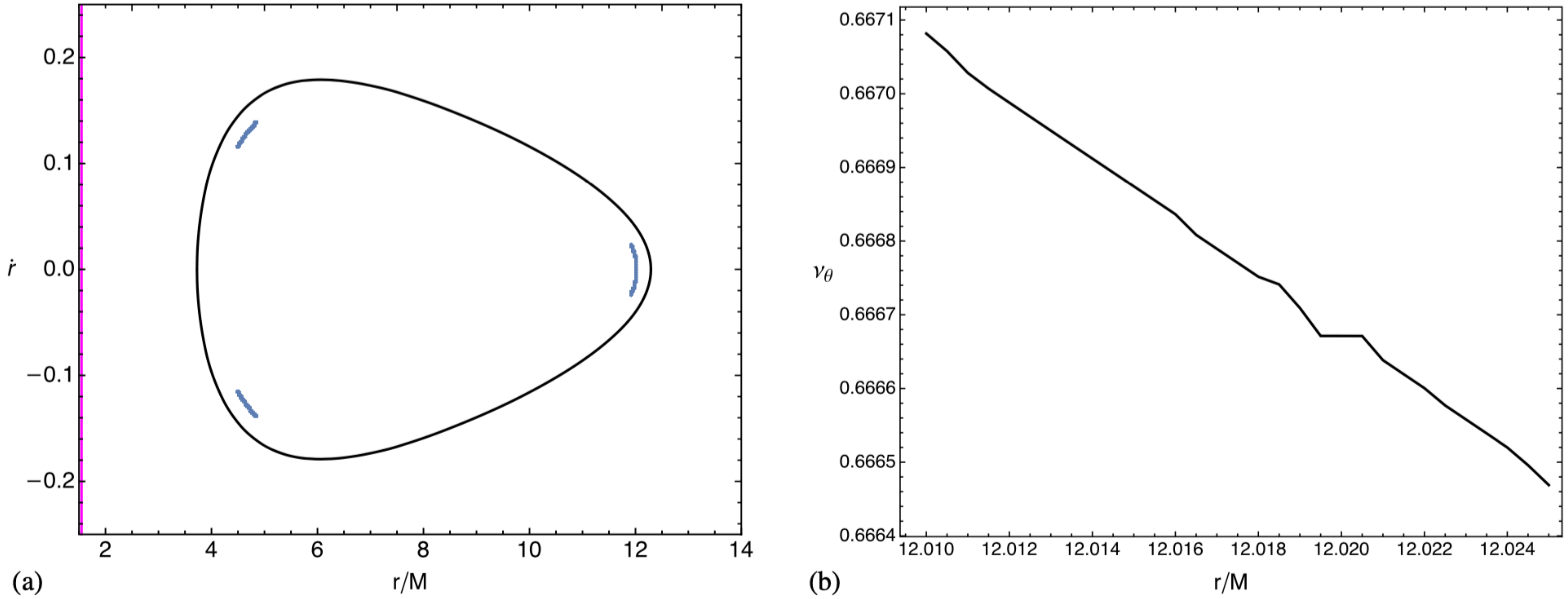

FIG. 11. (a) The $2/3$ Birkhoff islands for the 3PN effective metric for $a = 0.78\ M$ and $\eta = 0.01$. The initial conditions for the islands are $E = 0.942$, $L_z = 2.87\ M$, and $(r_0, y_0, \dot{r}_0) = (12.02M, 0, 0)$. The magenta line indicates the event horizon. (b) The rotation curve drawn along a horizontal line that crosses the rightmost branch of the islands. The plateau with $\nu_\theta = 2/3$ can be identified.

Conclusion

- In this work, we find a reliable way to check the (non-)integrability of inspiral dynamics of spinning binary.
- Adopt 2PN EOB formalism and the Ponicare-Birkhoff map, we can conclude that the 2PN inspiral dynamics of spinning binary is chaotic.
- The chaotic behaviors locate on some isolated islands in phase space.
- The compactness of the Birkhoff islands is challenging for the detection of chaotic behaviors in the emitted gravitational waves.

Thanks for listening!